ALD HfO_2 and Al_2O_3 as MIM Capacitor Dielectric for GaAs HBT Technology

Jiro Yota

GaAs Technology, Skyworks Solutions, Inc.
2427 W. Hillcrest Drive, Newbury Park, CA 91320, USA
jiro.yota@skyworksinc.com

Hafnium dioxide (HfO_2) and aluminum oxide (Al_2O_3) films have been deposited using atomic layer deposition (ALD) method and have been evaluated and used as metal-insulator-metal (MIM) capacitor dielectric in GaAs hetero-junction bipolar transistor (HBT) technology. The results show that the capacitor with 62 nm of ALD HfO_2 resulted in a capacitance density of 2.73 fF/μm^2, while that with 59 nm of ALD Al_2O_3 resulted in a capacitance density of 1.55 fF/μm^2. This capacitance density increased, when the temperature was increased from 25 to 150°C. There was no significant change in capacitance density of these ALD films, when the applied voltage was varied from -5 to +5 V and when the frequency was increased from 1 kHz to 1 MHz. The breakdown voltage of the ALD hafnium dioxide and aluminum oxide films was measured to be at 34 V and 41 V, respectively. As the temperature was increased from 25 to 150°C, the breakdown voltage of both films decreased, while the leakage current increased. These results show that both ALD HfO_2 and Al_2O_3 are compatible with, and suitable as MIM capacitor dielectric in GaAs HBT technology and can be adjusted to meet the specific application and requirements of the GaAs devices and designs.

Introduction

Due to the increasing demand for capacity and due to the increasing complexity and functionality of devices and designs, the die size in semiconductor wafer manufacturing must be reduced. One of the methods to reduce the design and die size is to increase the capacitance density and/or reducing the area of the metal-insulator-metal (MIM) capacitor, which is a key passive component in GaAs applications. Excluding the areas of the bond pad and scribe streets, MIM capacitors could consume up to 35% of the die area in many GaAs circuit designs (1,2). Increasing the capacitance density of the MIM capacitors in these designs will allow capacitor area reduction, which in turn will result in die size reduction. Furthermore, higher capacitance density will allow the integration of off-chip capacitors on the chip itself, thereby reducing the bill-of-materials in a multi-chip module.

The film and electrical characteristic requirements of a MIM capacitor for many GaAs applications, such as those fabricated using GaAs hetero-junction bipolar transistor (HBT) technology, are in many cases different from those of most silicon CMOS digital applications. In addition to high capacitance density requirement, the GaAs MIM capacitors also require low leakage current and high breakdown voltage. This is because

Presented at the Symposium on Graphene, Ge/III-V, and Emerging Materials for Post CMOS Applications 5 of the 2013 Electrochemical Society Meeting, Toronto, May 2013

in many GaAs designs, the operating voltage is typically high and the output voltage swings of the transistor can be 20 V or higher (1-3). Therefore, there are only a few available materials with a certain thickness that are compatible with GaAs processing and can be used to fabricate MIM capacitors. Furthermore, the thermal budget in the fabrication of many GaAs devices is limited, due to the degradation at high temperatures of the materials typically used in GaAs technologies. These include the metals used as contact materials to the devices and GaAs epitaxial layers (1,2,4-9). Therefore, in most cases, the highest allowable temperature for many GaAs backend process technologies is 300ºC, as compared to 400ºC or higher for many silicon process technologies (10,11). All these significantly limit the choices that are available for processes and materials to be used for fabrication of MIM capacitors in GaAs technology.

There are several methods that can be used to increase the capacitance density of a MIM capacitor. These include reducing the thickness of the capacitor dielectric and/or using a capacitor dielectric material with a higher dielectric constant. There have been many high dielectric constant materials evaluated as a MIM capacitor dielectric for semiconductor technologies (12-20). However, most of them have not been applied to or are not compatible with GaAs technology. The dielectric material most widely used as insulator of metal-insulator-metal capacitors in GaAs technology is silicon nitride (Si_3N_4), due to its compatibility with GaAs processing and good physical, chemical, and electrical characteristics (1,2,4,5,10,21-25). However, the dielectric constant of this silicon nitride is relatively low and ranges only from 6 to 7, depending on the deposition method, chemistry, and condition (1,4-6,10,11). There are a few other dielectric materials that have been considered and used as capacitor dielectric in GaAs technologies, including silicon dioxide (SiO_2), silicon oxynitride (SiON), and tantalum pentoxide (Ta_2O_5) (1,2,5,6,9,26-30). These films, along with silicon nitride, are typically deposited using physical vapor deposition (PVD) and plasma-enhanced chemical vapor deposition (PECVD) methods, both of which are compatible with GaAs processing and can be performed at 300ºC or lower. However, in general, these dielectric films do not possess or have all the GaAs MIM requirements and characteristics of high capacitance density, low leakage current, and high breakdown voltage (1,2,4,5,18,31,32).

In previous studies, we have developed high density MIM capacitors using atomic layer deposition (ALD) of aluminum oxide (Al_2O_3) and hafnium dioxide (HfO_2) as capacitor dielectric. We compared the MIM characteristics of these ALD films to those of a MIM capacitor with 63 nm PECVD Si_3N_4, which has a capacitance density of 0.93 $fF/\mu m^2$, a dielectric constant of 6.5, and a breakdown voltage of 73 V obtained in previous studies (1,2,4). In this study, we have further characterized electrically these ALD films of Al_2O_3 and HfO_2 as MIM capacitor dielectric for GaAs applications in hetero-junction bipolar (HBT) technology. The electrical characterization includes evaluating both the capacitance-voltage (C-V) and current-voltage (I-V) characteristics of the metal-insulator-metal capacitor, as a function of temperature, frequency, and capacitor area. This is important due to the fact that the GaAs devices may be operating at high temperatures, high voltages, at different frequencies, and may have capacitors that vary significantly in area within a design, and from design to design. This investigation will also discuss the factors and considerations that will determine which material is better suitable as MIM capacitor dielectric material for devices and designs manufactured using GaAs HBT technology.

Experimental

The aluminum oxide (Al_2O_3) and hafnium dioxide (HfO_2) films were deposited using atomic layer deposition (ALD) method in a Picosun Advanced SUNALE P-300 reactor. The precursors used for the deposition of the ALD Al_2O_3 are trimethyl aluminum (TMA), water, and O_3, while those used for deposition of the HfO_2 are tetrakisethylmethylamino hafnium (TEMAH), water, and O_3. The deposition temperature of the ALD Al_2O_3 and HfO_2 was 300ºC and 230ºC, respectively. The deposition thickness target of both films was 60 nm +/- 3 nm. In this study, both films were deposited on 6" GaAs wafers, including on device and bare test wafers. The device wafers were fabricated using GaAs hetero-junction bipolar transistor (HBT) technology, which includes the fabrication of multi-epitaxial devices, structures, and backend metal interconnections. Furthermore, these device wafers have metal-insulator-metal (MIM) capacitors, in addition to the hetero-junction bipolar transistor devices, which include the emitter, base, and collector. The MIM capacitor device on the GaAs HBT wafers includes the bottom metal electrode, the capacitor dielectric insulator, and the top metal electrode. Both these metal electrodes were deposited using evaporation method. The bottom metal electrode in this study was fabricated on top of a PECVD silicon nitride layer, which functions as a surface passivation and isolation layer on the GaAs wafers. This bottom metal electrode consists of 1 μm thick Au with a thin Ti adhesion layer on top, while the top metal electrode consists of 2 μm thick Au with a thin Ti layer at the bottom. The inter-metal dielectric used in this study is polybenzoxazole. The capacitor dielectric films were etched in BHF 10:1 solution to pattern the MIM capacitor devices.

In this study, a FilmTek 2000 reflectometer was used to measure the thickness and refractive index of the ALD HfO_2 and Al_2O_3 films. Furthermore, Focus-Ion Beam/Scanning Electron Microscopy (FIB/SEM) analysis was performed using a FEI Nova 600i instrument to evaluate the fabricated MIM capacitor structures, including the thickness and morphology of the dielectric films. Electrical characterization was performed by collecting both current-voltage (I-V) and capacitance-voltage (C-V) measurements using an Agilent B1500A semiconductor device analyzer, and using both a manual and automated probe station. The applied voltage for I-V characterization ranges from 0 to 50 V. Both the I-V and C-V measurements were performed on MIM capacitors with different areas, ranging from 100 to 10,000 μm^2, and at the temperatures of 25ºC and 150ºC. Capacitance characterization was also performed at different frequencies, ranging from 1 kHz to 1 MHz, and at different applied voltages, ranging from -5 to +5 V, and the temperatures of 25^oC and 150^oC. For all I-V measurements, the ground voltage is applied to the bottom metal electrode, while the bias voltage is applied to the top metal electrode.

Results and Discussion

Thickness, Refractive Index, and FIB/SEM Analysis

In order to obtain the film thickness and refractive index, the ALD HfO_2 and Al_2O_3 films were deposited on GaAs bare test wafers. The film thickness of the ALD aluminum oxide and hafnium dioxide films was measured to be 59 and 62 nm, respectively. The measured refractive index of the ALD aluminum oxide was 1.654,

while that of hafnium dioxide was 1.973. For FIB/SEM analysis and electrical characterization, the films were deposited on GaAs HBT device wafers. Figure 1 shows the FIB/SEM image of the metal-insulator-metal capacitor manufactured using GaAs HBT technology, along with the hetero-junction bipolar transistor, comprising the base, emitter, and collector. The image also shows the bottom metal of the MIM capacitor device being connected to the base of the transistor. Figures 2 (a) and (b) show the higher magnification FIB/SEM images of the MIM capacitor with 62 nm of ALD HfO_2 and 59 nm of ALD Al_2O_3, respectively, sandwiched between the top and bottom metal electrodes. It can be seen that the underlying, 1 μm thick, and evaporated bottom metal electrode of the MIM capacitor has high surface roughness. However, both capacitor dielectric insulator films show good conformality, when deposited on this rough, underlying metal surface. The good film conformality of these ALD films will lead to more uniform insulator thickness across the MIM capacitor and across the die, and within wafer and from wafer to wafer, resulting in more uniform capacitance, leakage current, and breakdown characteristics of the capacitor.

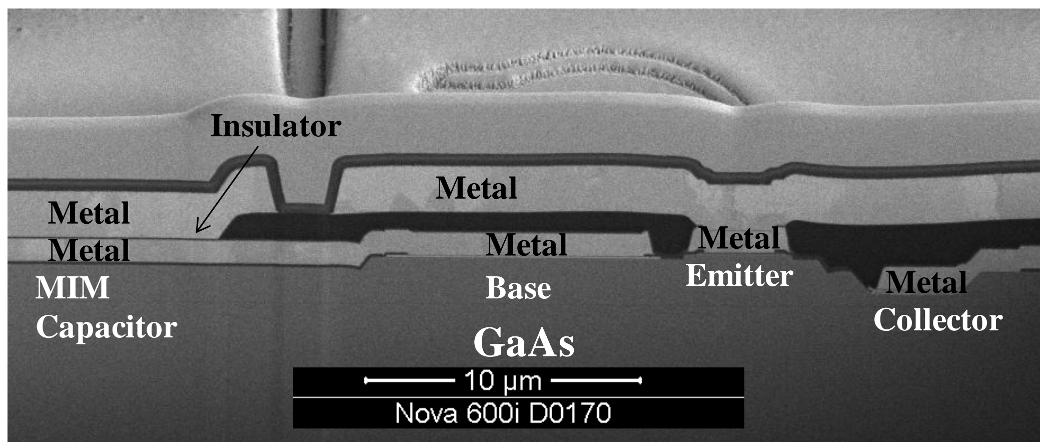

Figure 1. FIB/SEM image of a metal-insulator-metal (MIM) capacitor, connected to the base of a GaAs hetero-junction bipolar transistor, manufactured using GaAs HBT technology.

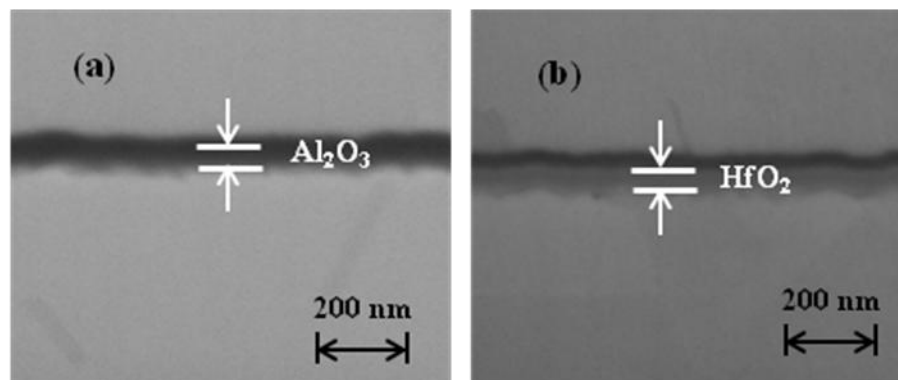

Figure 2. FIB/SEM images of GaAs MIM capacitors with (a) ALD Al_2O_3 and (b) ALD HfO_2 as capacitor dielectric, sandwiched between the top and bottom metal electrodes.

Capacitance Characterization

In order to evaluate the capacitance characteristics of the dielectric insulator films of the MIM capacitor, capacitance-voltage (C-V) measurements were performed. Figure 3 shows the capacitance density obtained from the MIM capacitor with an area of 4055 μm^2 and with capacitor dielectric insulator of 59 nm of ALD Al_2O_3 and 62 nm ALD HfO_2. As can be seen, the ALD HfO_2 has a capacitance density of 2.73 fF/μm^2, which is 76% higher than that of ALD Al_2O_3 with a capacitance density of 1.55 fF/μm^2. The capacitance density of both of these films is significantly higher than the capacitance density of 0.93 fF/μm^2 of a 63 nm PECVD Si_3N_4 obtained previously (1,2,4).

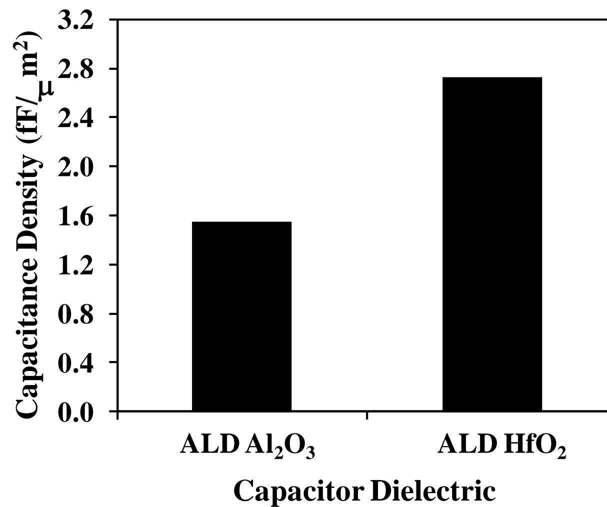

Figure 3. The capacitance density of MIM capacitors with 59 nm of ALD Al_2O_3 and 62 nm of ALD HfO_2 as capacitor dielectric.

Figure 4 shows the capacitance of MIM capacitors with both ALD films with capacitor areas ranging from 100 μm^2 to 10,000 μm^2. As shown, the capacitance of both films increases linearly with increasing capacitor area, indicating that the simple capacitor parallel-plate model can be used to model and approximate the MIM capacitor. Based on this model, the dielectric constant of the ALD Al_2O_3 and ALD HfO_2 is calculated to be 10.3 and 19.1, respectively, and which is shown in Figure 5. The dielectric constant of both ALD Al_2O_3 and HfO_2 films obtained in this study may not be as high as those obtained from similar and other high dielectric constant materials evaluated in previous studies (12-20). This may be caused by the different substrate and cathode metals used, by the different ALD deposition conditions used, and by the different processes performed before and after the deposition. All of these were performed in order for the processes and materials to be compatible with GaAs processing and are known to affect the dielectric constant and other characteristics of the MIM capacitor (18-20). However, to our knowledge, the dielectric constant of these ALD HfO_2 and Al_2O_3 films is still higher than that of any previously reported MIM capacitor dielectric material used in any GaAs technologies. When compared to the dielectric constant of 6.5 reported for PECVD Si_3N_4 (1,2,4), the dielectric constant of ALD HfO_2 is higher by 194%, while that of ALD Al_2O_3 is higher by 58%.

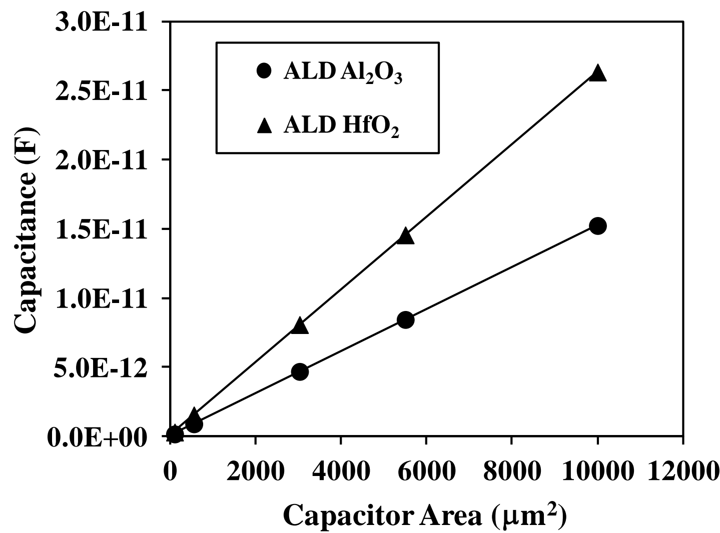

Figure 4. The capacitance of MIM capacitors with 59 nm of ALD Al_2O_3 and 62 nm of ALD HfO_2 as capacitor dielectric, as a function of area.

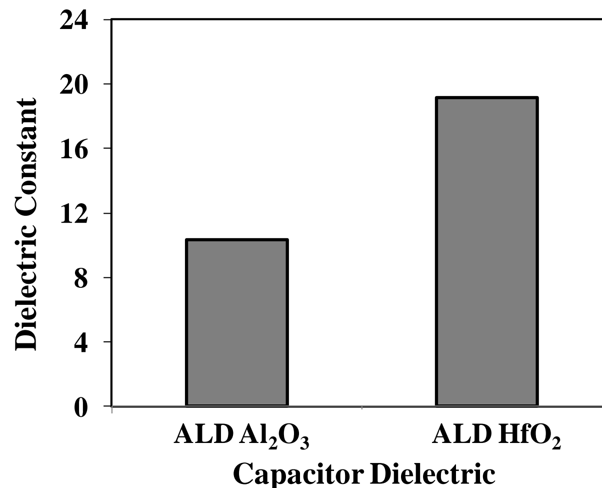

Figure 5. The dielectric constant of ALD Al_2O_3 and ALD HfO_2.

Since most GaAs devices may be operating at high temperatures, it is important to investigate the capacitance characteristics at a high temperature. The dependence of the capacitance density on the applied voltage and temperature of the MIM capacitor with the two ALD capacitor dielectrics is shown in Figures 6 and 7. As can be seen, the capacitance density of a MIM capacitor with ALD Al_2O_3 and with ALD HfO_2 did not vary significantly when the applied voltage was varied from -5 to 5 V. However, an increase in temperature from 25 to 150ºC resulted in an increase in the capacitance density of MIM capacitor with ALD Al_2O_3 from 1.55 to 1.59 fF/μm^2 (or an increase of 2.5%). The MIM capacitor with ALD HfO_2 also increased in capacitance density from 2.73 to 2.81 fF/μm^2 (or an increase of 2.9%), when the temperature was increased from 25 to 150ºC.

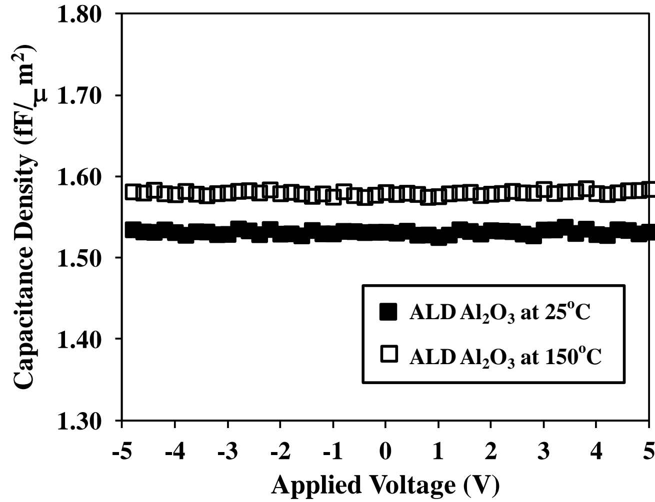

Figure 6. The capacitance density of a MIM capacitor with 59 nm of ALD Al_2O_3 as capacitor dielectric at 25°C and 150°C.

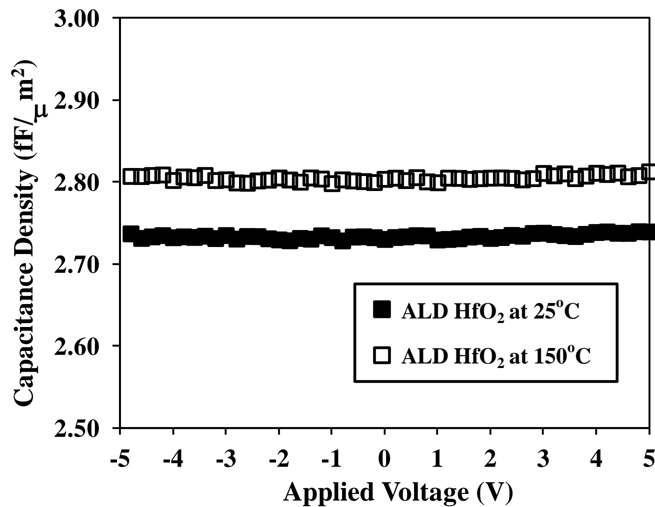

Figure 7. The capacitance density of a MIM capacitor with 62 nm of ALD HfO_2 as capacitor dielectric at 25°C and 150°C.

Figures 8 and 9 show the capacitance characteristics of the MIM capacitors with ALD Al_2O_3 and with ALD HfO_2 as capacitor dielectric, when the frequency was increased from 1 kHz to 1 MHz, and the applied voltage was varied from -5 to +5 V. As can be seen, the capacitance density did not significantly change, as a function of frequency. Similarly, no change was observed, when the applied voltage was varied for both capacitor dielectric films.

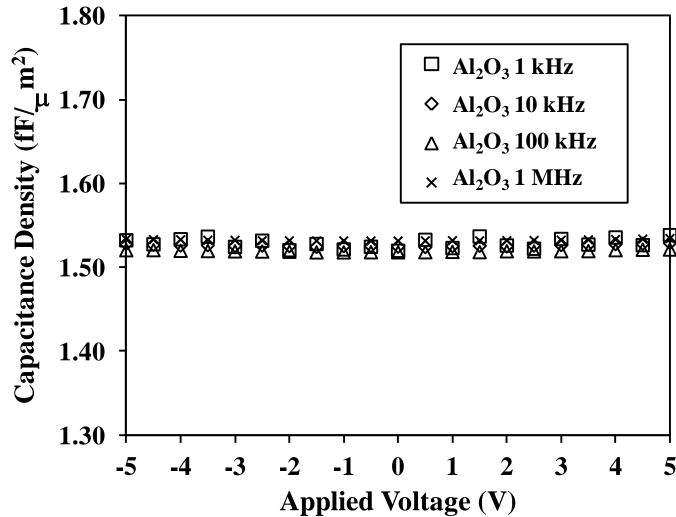

Figure 8. The capacitance density of a MIM capacitor with 59 nm of ALD Al_2O_3 as capacitor dielectric, as a function of frequency.

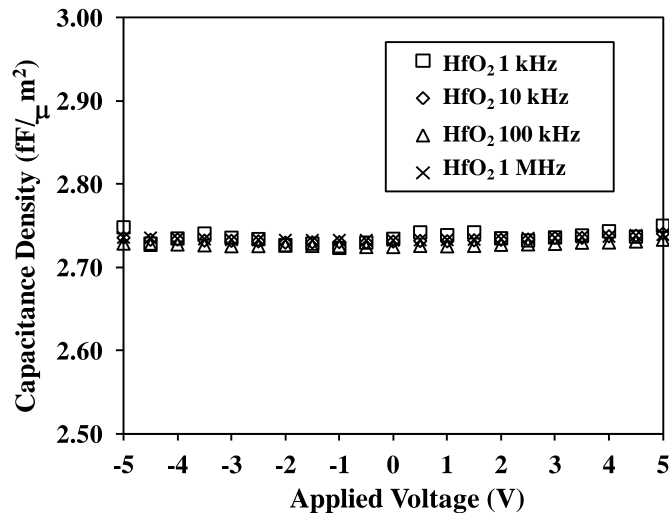

Figure 9. The capacitance density of a MIM capacitor with 62 nm of ALD HfO_2 as capacitor dielectric, as a function of frequency.

Leakage Current Characterization

Current-voltage characterization was performed to evaluate the leakage current characteristics of the MIM capacitors with ALD aluminum oxide and ALD hafnium dioxide capacitor dielectric. The measurements were performed on capacitors with different areas and at different temperatures. Figure 10 shows the I-V curve of the capacitor with an area of 4055 μm^2 using both films, as the applied voltage was increased

from 0 to 50 V and the temperature was increased from 25 to 150ºC. As can be seen, the capacitor with 59 nm ALD Al_2O_3 resulted in lower leakage current, as compared to the capacitor with 62 nm ALD HfO_2. The non-linear I-V behavior and different characteristics in certain voltage ranges of the ALD Al_2O_3 films in this study indicate that there may be multiple carrier conduction processes occurring, when the voltage was biased, including Schottky, Frenkel-Poole, and Fowler-Nordheim tunneling emissions (9,33,34). The ALD HfO_2 shows more linear I-V characteristics, possibly suggesting that there was only one carrier conduction process that is significant or dominant during the bias. Figure 10 also shows the I-V characteristics of both films as the temperature was increased from 25 to 150ºC. As expected, the capacitor leakage current increased, when the temperature was increased.

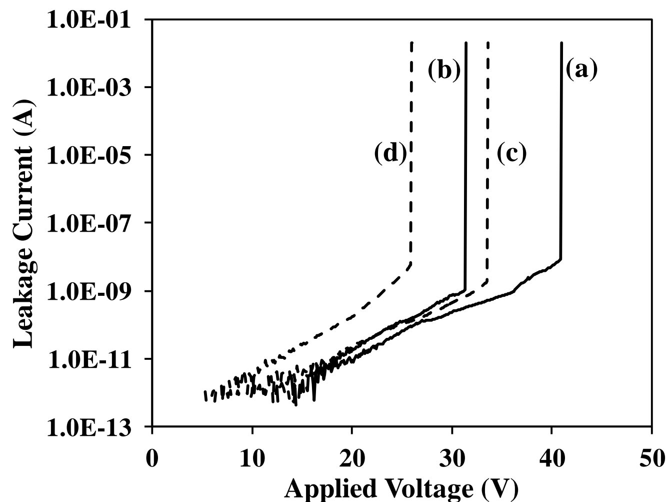

Figure 10. The I-V characteristics of MIM capacitors with 59 nm of ALD Al_2O_3 at (a) 25°C and (b) 150°C, and with 62 nm of ALD HfO_2 at (c) 25°C and (d) 150°C.

The dependence of capacitor leakage current on MIM capacitor area is also important, as the capacitor area in GaAs circuit designs can vary significantly. A capacitor with a larger area results in higher leakage current, and which may result in earlier capacitor breakdown. Figure 11 and Figure 12 show the I-V curves of MIM capacitor with ALD Al_2O_3 and ALD HfO_2, as a function of MIM capacitor area. As expected, the leakage current of both films significantly increased, when the capacitor area was increased from 100 to 10,000 μm^2.

Breakdown Characterization

The breakdown voltage characteristics were also obtained from C-V measurements. The breakdown voltage of MIM capacitors with 59 nm ALD Al_2O_3 and with 62 nm ALD HfO_2 are shown in Figure 13. As can be seen, the ALD Al_2O_3 has a higher breakdown voltage of 41 V, as compared to HfO_2, which has a breakdown voltage

of 34 V. As the temperature was increased from 25 to 150ºC, the breakdown voltage of ALD Al_2O_3 and HfO_2 decreased to 31 V and 26 V, respectively. This breakdown voltage of these films is higher than the possible voltage output swings in GaAs HBT technology, making them suitable for GaAs applications.

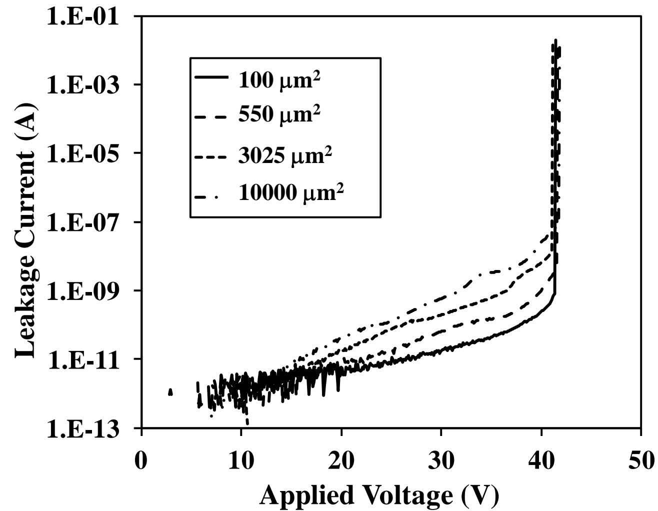

Figure 11. The I-V characteristics of MIM capacitors with 59 nm of ALD Al_2O_3 as capacitor dielectric, as a function of capacitor area.

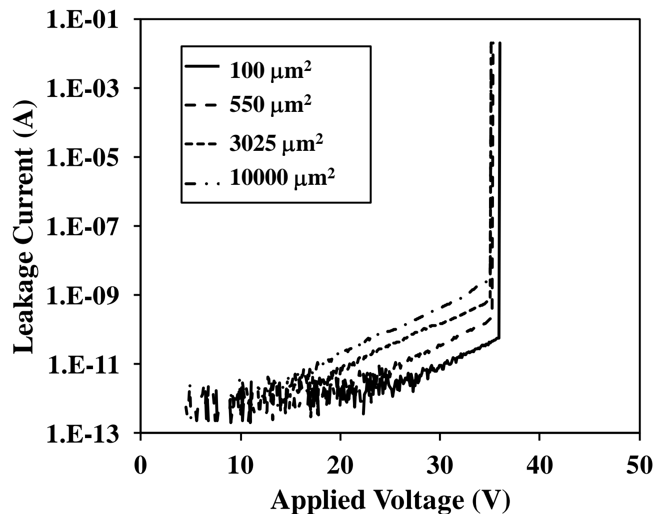

Figure 12. The I-V characteristics of MIM capacitors with 59 nm of ALD HfO_2 as capacitor dielectric, as a function of capacitor area.

Figure 14 shows the breakdown voltages of MIM capacitor with ALD Al_2O_3 and ALD HfO_2, as a function of MIM capacitor area. No significant difference was observed in the breakdown voltage of both these films, when the capacitor area was increased from 100 to 10,000 μm^2. Figure 15 shows the calculated breakdown field of both films in this study. The data show that the breakdown field of ALD Al_2O_3 is 7.0 MV/cm, while that of ALD HfO_2 is 5.4 MV/cm. This breakdown field is lower than the 11.6 MV/cm reported for PECVD Si_3N_4 (1,2,4,10,11).

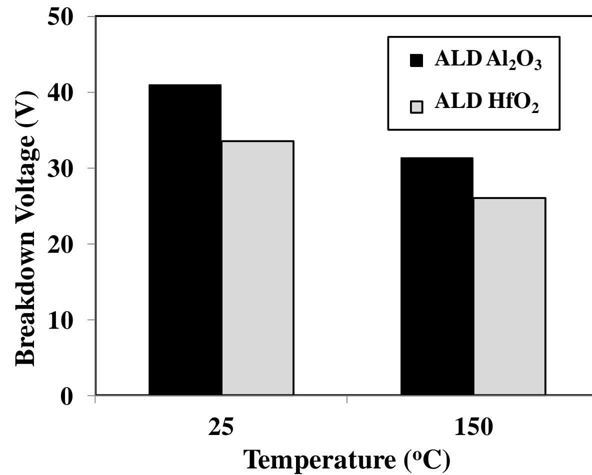

Figure 13. The breakdown voltage of MIM capacitors with 59 nm of ALD Al_2O_3 and with 62 nm of ALD HfO_2 at 25°C and 150°C.

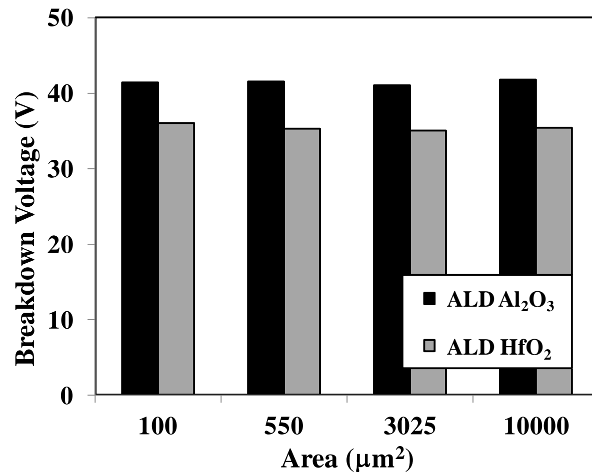

Figure 14. The breakdown voltage of MIM capacitors with 59 nm of ALD Al_2O_3 and with 62 nm of ALD HfO_2, as a function of capacitor area.

MIM Dielectric for GaAs HBT Technology

Based on the electrical characterization results, a MIM capacitor with 59 nm ALD Al_2O_3 and with 62 nm ALD HfO_2 films as a capacitor dielectric have significantly higher capacitance density that that with PECVD Si_3N_4, which is typically used in GaAs process technology. Furthermore, the breakdown voltage of both ALD films is also higher than the output voltage swings that may be experienced and the operating voltage that is typically used in GaAs HBT devices. These data show that both of these films are suitable for, and can be used as MIM capacitor dielectric in GaAs HBT technology. The selection of the film depends on what the specific application and electrical requirements and specifications of the GaAs devices and designs are. These requirements and specifications include how high the capacitance density is, how low the leakage current is, and how high the capacitor breakdown voltage is of the capacitor dielectric film at a specific condition, in addition to how the electrical characteristics change with different temperatures, different frequencies, and for different MIM capacitor areas.

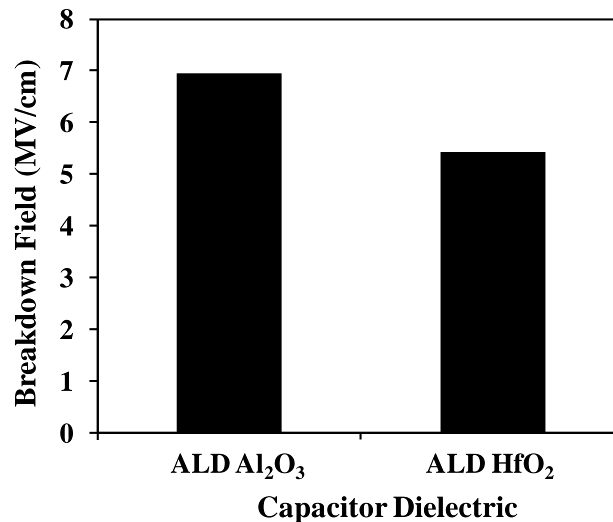

Figure 15. The breakdown field of ALD Al_2O_3 and ALD HfO_2.

In order to achieve the required and desired electrical characteristics of these MIM capacitors, the thickness of the two ALD capacitor dielectric insulator films can be adjusted and modified. For instance, the thickness of each film can be reduced in order to achieve higher capacitance density. However, this will also result in higher leakage current, in addition to lower breakdown voltage, and which is proportional to the thickness reduction. Conversely, the thickness can be increased in order to obtain higher breakdown voltage and lower leakage current. However, this will result in lower capacitance, and which is inversely proportional to the thickness of the film. Therefore, these ALD capacitor dielectric films can each be specifically tailored to meet some or all electrical requirements, including capacitance density, breakdown voltage, leakage current, and other electrical characteristic requirements of the GaAs device and circuits. Depending on the results and specific GaAs device application, one film may be better and more suitable that the other film as MIM capacitor dielectric insulator film for GaAs HBT technology.

Conclusions

ALD HfO_2 and Al_2O_3 have been evaluated and used as a MIM capacitor dielectric fabricated using GaAs HBT technology. The results show that the capacitor with 62 nm of ALD HfO_2 and 59 nm of ALD Al_2O_3 resulted in a high capacitance density of 2.73 $fF/\mu m^2$ and 1.55 $fF/\mu m^2$, respectively. This capacitance density increased, when the temperature was increased from 25 to 150°C and no significant change in capacitance was observed, when the applied voltage was varied from -5 to +5 V and when the frequency was increased from 1 kHz to 1 MHz. The breakdown voltage of the ALD hafnium dioxide and aluminum oxide films was measured to be at 34 V and 41 V, respectively. When the temperature was increased from 25 to 150°C, the breakdown voltage of both films decreased, while the leakage current increased. The results show that both ALD HfO_2 and Al_2O_3 are compatible with and suitable as MIM capacitor dielectric in GaAs HBT technology and can be adjusted to meet the specific application and requirements of the GaAs devices and designs.

Acknowledgments

The author would like to acknowledge Ravi Ramanathan, Mike Sun, Benny Do, Mark Banbrook, and David Tuunanen of Skyworks Solutions, Inc., and Jay Sasserath and Frank Lowry from LabTec for their help in this study.

References

1. J. Yota, H. Shen, and R. Ramanathan, *J. Vac. Sci. Technol. A*, **31** (1), 01A134-1 (2013).
2. J. Yota, R. Ramanathan, K. Kwok, J. Arreaga, T. Ko, and H. Shao, in *Proc. 2005 Electrochemical Society Meeting: State-of-the-Art-Program on Compound Semiconductors (SOTAPOCS),* PV 2005-04, p. 315, The Electrochemical Society Proceeding Series, Pennington, NJ (2005).
3. P. Leber, M. Hollmer, D. Schrade-Kohn, J. Thorpe, E. Behtash, H. Blanck, and H. Schumacher, in *2011 CS MANTECH Tech. Digest*, pp. 275-278 (2011).
4. J. Yota, R. Ramanathan, J. Arreaga, P. Dai, C. Cismaru, R. Burton, P. Bal, and L. Rushing, in *2003 GaAs MANTECH Tech. Digest*, pp. 65-68 (2003).
5. R. Williams, *Modern GaAs Processing Methods*, Artech House, Boston (1990).
6. S.K. Gandhi, *VLSI Fabrication Principles, Silicon and Gallium Arsenide*, New York, John Wiley (1983).
7. J. Yota, H. Ly, R. Ramanathan, M. Sun, D. Barone, T. Nguyen, K. Katoh, M. Ohe, R. L. Hubbard and K. Hicks, *IEEE Trans. Semicond. Manuf.*, **20**, 323 (2007).
8. J. Yota, *J. Electrochem. Soc.,* **156**, G173 (2009).
9. W. Liu, *Handbook of III-V Heterojunction Bipolar Transistors*, New York, John Wiley (1998).
10. S.M. Sze, *VLSI Fabrication Technology*, McGraw-Hill, New York (1988).
11. S. Wolf and R.N. Tauber, *Silicon Processing for the VLSI Era Volume 1 - Process Technology*, Lattice Press, Sunset Beach (1986).

12. D. Suh and J. Kang, *J. Vac. Sci. Technol. B*, **20**, 717 (2002).
13. C. Durand, C. Vallee, V. Loup, O. Salicio, C. Dubordieu, S. Blonkowski, M. Bonvalot, P. Holliger, and O. Joubert, *J. Vac. Sci. Technol. B*, **22**, 655 (2004).
14. A. Krause, W. Weber, A. Jahn, K. Richtter, D. Pohl, B. Rellinghause, U. Schroder, J. Heitmann, and T. Mikolajick, *J. Vac. Sci. Technol. B*, **29**, 01AC07-1 (2011).
15. B. C. Lai and J. Y. Lee, *J. Electrochem. Soc.,* **146**, 266 (1999).
16. J. Robertson, *Eur. Phys. J. Appl. Phys*., **28**, 265 (2004).
17. M. Hota, S. Mallik, C. K. Sarkar, and C. K. Maiti, *J. Vac. Sci. Technol. A***, 29**, 01AC06-1 (2011).
18. T. H. Phung, D. K. Srinivasan, P. Steinmann, R. Wise, M. B. Yu, Y. C. Yeo, and C. Zhu, *J. Electrochem. Soc*., **158**, H1289 (2011).
19. T. J. Park, J. H. Kim, J. H. Jang, C. S. Hwang, H. D. Kang, Y. K. Chung, and Y. S. Oh, *J. Electrochem. Soc*., **158**, G1 (2011).
20. C. Wenger, M. Lukosius, H.J. Mussig, G. Ruhl, S. Pasko, and C. Lohe, *J. Vac. Sci. Technol. B*, **27** (1), 286 (2009).
21. J. Yota, J. Hander, and A.A. Saleh, *J. Vac. Sci. Technol. A,* **18** (2), 372 (2000).
22. G. Dandrova, J.M. Beall, and K.D. Decker, *ECS Trans*., **6** (3), 397 (2007).
23. C. Nevers, A.T. Ping, T. Rivers, S. Varma, F. Pool, M. Minkoff, E. Etzkorn, and O. Berger, in *2009 CS MANTECH Tech. Digest*, pp. 117-120 (2009).
24. T. Kagiyama, Y. Tosaka, R, Yamabi, and H. Yano, in *2007 CS MANTECH Tech. Digest*, pp. 51-54 (2007).
25. M.N. Osman, A. Dolah, A.I.A. Rahim, M.R. Yahya, and A.D.A. Mat, in *Proc. IEEE International Conference on Semiconductor Electronics*, pp. 515-510 (2006).
26. C. Whitman and M. Meeder, in *Reliability of Compound Semiconductors Workshop*, pp. 91-102 (2004).
27. J. Scarpulla, D.C. Eng, S.R. Olson, and C.S. Wu, in *Proc. 1999 IEEE Reliability Physics Symposium*, pp. 128-137 (1999).
28. M.E. Elta, A. Chu, L.J. Mahoney, R.T. Cerretani, and W.E. Courtney, *IEEE Dev. Lett.* **3** (5), 127 (1982).
29. H.B. Profijt, S.E. Potts, M.C.M. van der Sanden, and W.M.M. Kessels, *J. Vac. Sci. Technol. A*, **29**, 00801-1 (2011).
30. S.B.S. Heil, F. Roozenboom, M.C.M. van der Sanden, and W.M.M. Kessels, *J. Vac. Sci. Technol. A*, **26**, 472 (2008).
31. A.S. Zoolfakar and H. Hasim, in *Proc. IEEE International Conference on Semiconductor Electronics (ICSE)*, pp. 445-449 (2008).
32. B. Hudec, K. Husekova, E. Dobrocka, J. Aarik, R. Rammula, A. Kasikov, A. Tarre, A. Vincze, and K. Frohlich, *J. Vac. Sci. Technol. B*, **29**, 01AC09 (2011).
33. K. Chiang, C.C. Huang, G.L. Chen, W.J. Chen, H.L. Kao, A. Chin, and S.P. McAlister, *IEEE Trans. Electron. Dev*, **53**, 2312 (2006).
34. S.M. Sze, *Physics of Semiconductor Devices*, John Wiley and Sons, New York (1981).